Instrumental and Process Considerations for the Fabrication of Silicon-on-Insulators (SOI) Structures by Plasma Immersion Ion Implantation

Paul K. Chu, *Member, IEEE*, Shu Qin, *Senior Member, IEEE*,
Chung Chan, *Fellow, IEEE*, Nathan W. Cheung, and Ping K. Ko, *Fellow, IEEE*

***Abstract*— Plasma immersion ion implantation (PIII) has recently been shown to be a viable method to fabricate silicon-on-insulator (SOI) materials using either the SPIMOX (separation by plasma implantation of oxygen) or the ion cut/wafer bonding method. We have recently modified and characterized a new generation plasma immersion ion implanter for SOI fabrication, and this paper will discuss some of the instrumental and processing issues, including the plasma source, mean free path consideration, and dc sheath characteristics.**

NOMENCLATURE

j_c	Ion current density.
m	Mass of the ion.
n_i	Ion density.
q	Electron charge.
s or s_c	Steady-state sheath thickness.
s_0	Ion-matrix sheath thickness.
T_e	Electron temperature.
u_B	Bohm acoustic speed.
ε_0	Permittivity of free space.
λ_i	Ion-neutral mean free path of the charge transfer collision.
σ_i	Cross section of charge transfer collision.
ω_{pe}	Electron plasma frequency.
ω_{pi}	Ion plasma frequency.

I. INTRODUCTION

SILICON-ON-INSULATOR (SOI) offers many inherent advantages over silicon substrates for low-power high-speed deep-submicrometer CMOS (complementary metal oxide semiconductor) integrated circuits [1]–[3]. The two commercial ways to fabricate SOI wafers, namely, SIMOX (separation by implantation of oxygen) and BESOI (bonded and etch-back) SOI, are quite expensive because of the long implantation time for the SIMOX process and the need to use two wafers to form a single SOI wafer in BESOI. Recently, a method called SMART-CUT^{TM} or ion cut was proposed by SOITEC, making use of wafer cleavage after hydrogen implantation and subsequent wafer bonding [4]. This technique is potentially cheaper than the conventional BESOI process because one of the wafers can be recycled. The materials cost of SOI can be further reduced if an alternative way can be found to reduce the time required to implant a high enough dose of oxygen (SPIMOX) or hydrogen (ion-cutting).

Plasma immersion ion implantation (PIII) is a burgeoning technique offering many applications in materials and semiconductor processing [5]–[7]. In PIII, the sample is immersed in a plasma shroud from which ions are extracted and accelerated through a high-voltage sheath into the target. The dose rate can be as high as 10^{16} ions $\cdot$ cm^2 $\cdot$ s^{-1}, which is equivalent to ten monolayers of implanted atoms per second and at least an order of magnitude higher than that of a conventional ion implanter. Since the entire wafer is implanted simultaneously, the implantation time is independent of wafer size, thereby offering an extremely attractive approach for 300-mm wafers. The use of PIII to synthesize SOI materials has been investigated, and the results are very encouraging [8]–[12]. In spite of the tremendous potential, the development of commercial PIII instrumentation has not caught up. We recently installed two new generation plasma immersion ion implanters. The first one was designed for general and metallurgical applications [13], and the second one that was used to investigate SOI fabrication parameters for this work was acquired from Waban Technology, Inc. and modified by the research staff at the City University of Hong Kong. Fig. 1 shows a schematic of the system configuration of the second prototype with the integration of the radio frequency (RF) plasma source. It consists of a chamber with a multipolar magnetic confinement structure, 13.45-MHz RF power amplifier, tuning matching network, inductively coupled plasma (ICP) antenna unit, vacuum and gas handling, wafer temperature control, and high-voltage power supply (dc or pulse generator). The vacuum chamber is 66 cm (26 in) in diameter and 80 cm (32 in) high. The large processing chamber is designed to accommodate a 300-mm (12-in) wafer. A multipolar bucket structure is used for plasma confinement in the chamber.

We have investigated the operational phase-space of the SPIMOX process [14], and in this paper, we will describe the instrumental and processing aspects of the synthesis of SOI materials by both the SPIMOX and PIII ion cut techniques [15].

Manuscript received May 6, 1997; revised September 4, 1997. This work was supported by City University of Hong Kong Grant 7000730 and Hong Kong Research Grants Council Contracts 8730005 and 9040220.

P. K. Chu is with the Department of Physics and Materials Science, City University of Hong Kong, Kowloon, Hong Kong.

S. Qin and C. Chan are with the Department of Electrical Engineering, Northeastern University, Boston, MA 02115 USA.

N. W. Cheung is with the Department of EECS, University of California, Berkeley, CA 94720 USA.

P. K. Ko is with the School of Engineering, Hong Kong University of Science and Technology, Clear Water Bay, Kowloon, Hong Kong.

Publisher Item Identifier S 0093-3813(98)00698-5.

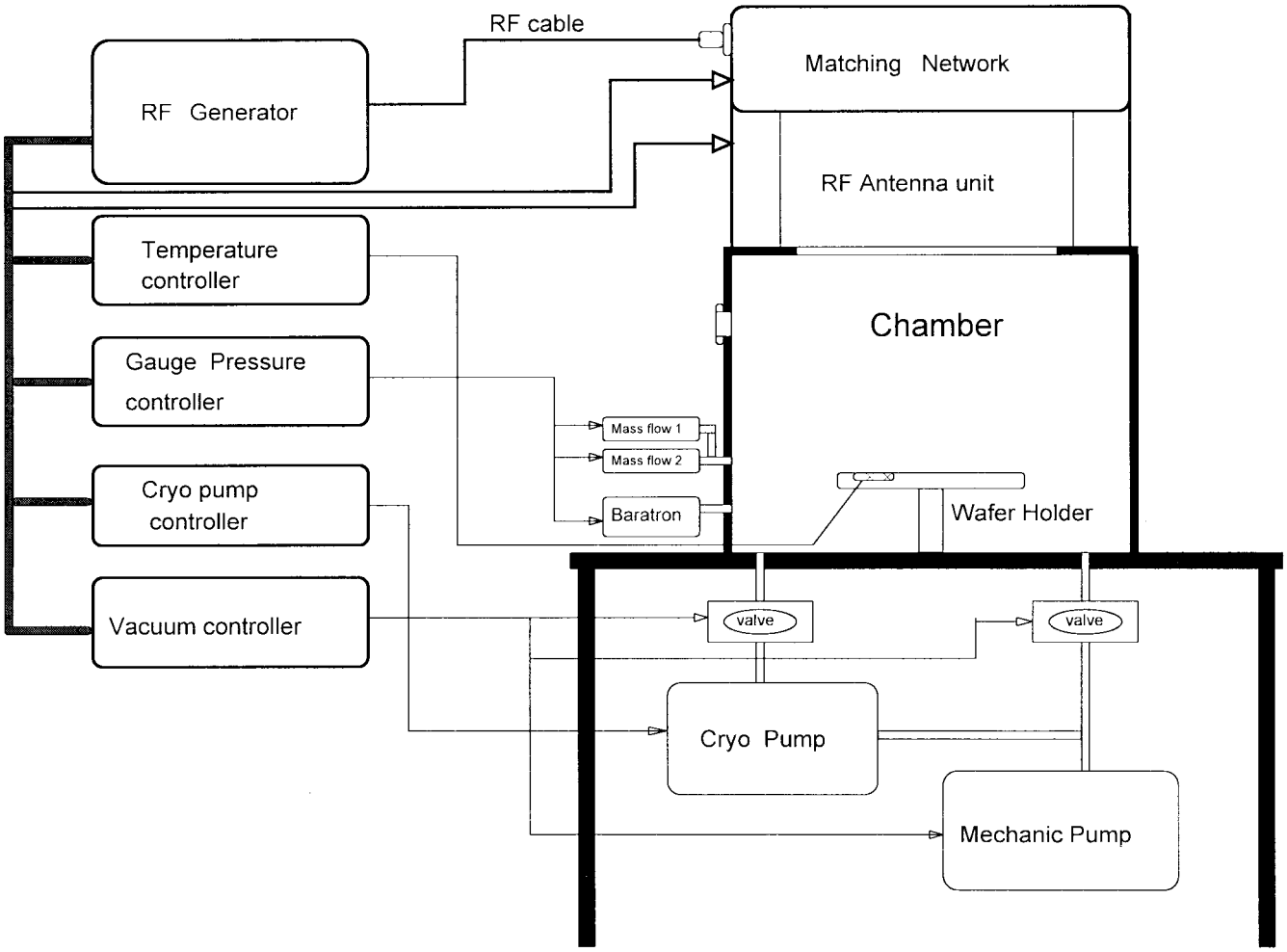

Fig. 1. Schematic of the prototype system.

II. Characteristics of Plasma Source

One of the most important instrumental parameters for the successful fabrication of SOI materials is plasma uniformity which has a direct impact on the dose uniformity. This is more important for SPIMOX than ion-cut/wafer bonding because, in SPIMOX, the buried oxide and the surface epitaxial layer must be very uniform laterally, whereas in the latter process, the implanted hydrogen dose just needs to be uniform enough to cause continuous cracking along the wafer plane. Minor uneven cracking is acceptable because most of the materials will be polished away to leave a thin epitaxial layer on the bonded wafer. The proprietary plasma source used in this study is based on a patented source design [16]. The source was designed to accomplish superior SOI implant processing characteristics over large substrate areas including excellent ion density uniformity ($\sim$4% across a 400-mm-diameter wafer) with a reasonable ion density ($\sim 10^{10}/\mathrm{cm}^3$), wide ranges of operating pressure (0.1–100 mTorr), and ease of operation.

To characterize the performance of the plasma source, a Langmuir probe with a quarter-in-diameter tantalum disk tip was used for plasma measurements. Biasing this tip allows the collection of electrons or ions. Electron temperatures of $\sim$2–4 eV and plasma potential of $\sim$15–25 V, which depended on the pressure, RF power, and position in the chamber, were obtained from the Langmuir probe *I–V* measurements for a nitrogen plasma.

Fig. 2 displays the relationship of the plasma density versus working pressure for different axial distance to source when the RF power is 800 W. Figs. 3 and 4 show the plasma density radial profiles in the chamber for different axial-to-source distances when the RF power is 800 W and the pressure is 1 and 2 mTorr, respectively. At a pressure of 2 mTorr and RF power of 800 W, the ion density uniformity is within 1.2, 2.3, 20.9, and 37% across 150 mm (6 in), 200 mm (8 in), 300 mm (12 in), and 400 mm (16 in) wafers, respectively. At a pressure of 1 mTorr, excellent plasma density uniformity can be achieved at an axial distance of 20 cm to source. When the RF power is 800 W, the ion density uniformity is within 2, 4, 4, and 4% across 150 mm (6 in), 200 mm (8 in), 300 mm (12 in), and 400 mm (16 in) wafers, respectively. Although a better uniformity is observed at higher pressure (2 mTorr) for a target which is smaller than a 200-mm wafer, much better uniformity is achieved at lower pressure for a target larger than 300 mm. Since we see no fundamental scaling problem in the plasma source, the ion density uniformity of 4% across 406.4 mm (16-in-diameter silicon wafer) is a great improvement from 15% across a 300×400 mm^2 panel as claimed by a Nissin ion shower machine.

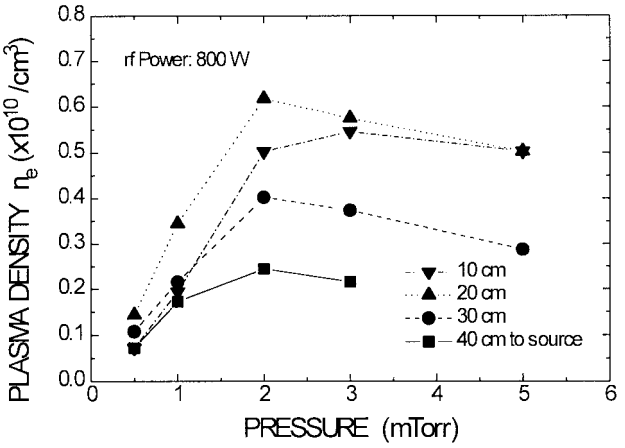

Fig. 2. Plasma density versus working pressure for different axial distance to source when RF power is 800 W.

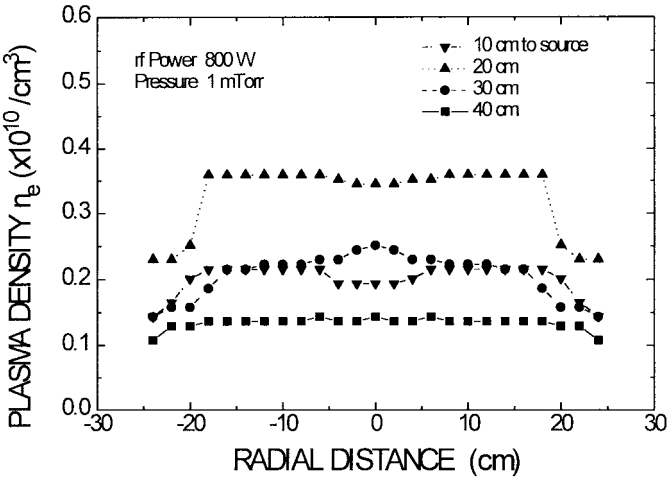

Fig. 3. Plasma density radial profiles in chamber for different axial distance to source at 800-W RF power and 1-mTorr pressure.

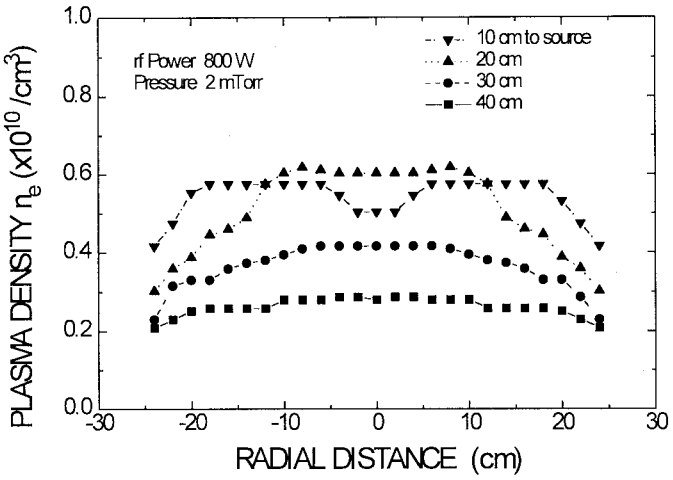

Fig. 4. Plasma density radial profiles in chamber for different axial distance to source at 800-W RF power and 2-mTorr pressure.

Presently, the maximum ion density is mostly limited by the RF power supply with 1000-W drive power (average power on each antenna is only 250 W). Higher ion density can be expected if higher RF power is applied to the source. However, for the SOI process, very high ion density is not desired due to the power limitation of the high-voltage power supply and the heat dissipation limitation on the wafer during the PIII process. Overheating of the wafer caused by high dose-rate and high-energy ion bombardment must be avoided for both the SPIMOX process using oxygen implantation as well as the ion-cut process using hydrogen or helium implantation.

III. PIII/SOI Process Considerations

The characteristics of the sheath during PIII process are very important for the optimal design of the PIII configuration and process control. For example, the sheath thickness is critical to the chamber design (chamber size $>$ sheath thickness plus target size for a stable plasma) and mono-energetic ion implantation ($s/\lambda_i < 1$ for collisionless plasma, where s is the sheath thickness and λ_i is the mean free path of ion-neutral charge exchange collision in the sheath). This is particularly important to the SPIMOX or ion-cutting processes because there are some special requirements. An as-implant profile with an ideal Gaussian distribution beneath the silicon surface is required for a good quality box structure. Therefore, monoenergetic implantation is desirable. The PIII process for SOI formation usually has a relatively thicker sheath because of two reasons. The first reason is that a high voltage (~ -50 to -100 kV) is required to attain a sufficiently large implantation depth, and the second reason is that the ion density is relatively small when the operating pressure is kept low in order to maintain a mean free path λ_i larger than the sheath thickness (see characteristics of the plasma source). Besides, the ion density needs to be kept at a relatively low level to stay below the maximum output power of the high-voltage power supply. However, the thicker sheath will directly conflict with the monoenergetic ion implantation ($s/\lambda_i < 1$) requirement if the process pressure can be kept at the lowest level. Therefore, the precise modeling and simulation of the sheath are very important in order to predict the sheath characteristics and to control the process conditions. Modeling and simulation of the sheath can also be used to predict doping results such as the implant dose and impurity profile.

IV. Monoenergetic Implant Requirements

A low operating pressure is required to meet collisionless conditions for monoenergetic implantation. Figs. 5 and 6 depict the relationship between the mean free path and the operating pressure for oxygen and helium plasmas, respectively. The mean free paths in oxygen and helium plasmas are 2 and 1.5 cm, respectively, when the pressure is 10 mTorr. They increase to 20 and 15 cm, respectively, when the pressure decreases to 1 mTorr, and further increase to 200 and 155 cm, respectively, when the pressure decreases to 0.1 mTorr.

Contrary to conventional PIII conditions, dc bias or quasi-dc bias (the flat part of each pulse is much longer than the rise time and fall time of the pulse) in lieu of pulse bias is required for monoenergetic implantation. It is because the ion-matrix sheath characteristics and the rise time, fall time of the high-voltage pulse, even in a collisionless plasma, will cause a broadened energy distribution of the implanted ions.

TABLE I
SHEATH THICKNESS, IMPLANT ION CURRENT, AND IMPLANT DOSE-RATE VERSUS THE DIFFERENT ION DENSITIES WHEN A DC BIAS OF −50 kV IS APPLIED

Ion Density ($/cm^3$)	Sheath Thickness* (cm)	Implant Ion Current** (A)		Implant Dose-Rate $\times 10^{15}$ ($/cm^2$ sec)	
		O^-	He^+	O^-	He^-
1×10^{9}	52.4	0.0101	0.0202	0.346	0.692
4×10^{9}	26.2	0.0404	0.0808	1.38	2.77
1×10^{10}	16.6	0.101	0.202	3.46	6.92
1×10^{11}	5.24	1.01	2.02	34.6	69.2

* One-dimensional results.

** Area (6 inch wafer) = 182.4 cm^2.

V. DC SHEATH CHARACTERISTICS

The dc sheath thickness can be characterized by the well-known Child–Langmuir Law of the space-charge-limited current in a one-dimension planar coordinate

$$j_c = \frac{4}{9}\varepsilon_0\sqrt{\frac{2q}{m}}\,\frac{V^{3/2}}{s^2} \tag{1}$$

and a steady-state ion current at the sheath edge with a Bohm acoustic speed $u_B = (qT_e/m)^{1/2}$

$$j_c = qn_i u_B \tag{2}$$

where j_c is the ion current density crossing the sheath edge, ε_o is the free-space permittivity, q is the ion charge, m is the ion mass, V is the absolute value of the applied potential, s is the sheath thickness, n_i is the ion density, and T_e is electron temperature in units of electron volts.

The steady-state sheath thickness can be obtained by solving (1) and (2) simultaneously, so that

$$s_c = s_0\sqrt{\frac{2}{9}}\left(\frac{2V}{T_e}\right)^{1/4} \tag{3}$$

in which s_o is the ion-matrix sheath defined as the sheath formed when $t = 0^+$, but t is longer than the electron response time ($\sim\omega_{pe}^{-1}$) and shorter than the ion response time ($\sim\omega_{pi}^{-1}$), and is given by

$$s_0 = \sqrt{\frac{2\varepsilon_0 V}{an_i}}. \tag{4}$$

From (3), we can see that, like ion-matrix sheath s_o, the dc sheath s_c, is independent of the ion species.

After the steady-state sheath is determined, the implant ion current, which is also a steady-state current, can be obtained directly from the Child–Langmuir Law

$$j_c = \frac{4}{9}\varepsilon_0\sqrt{\frac{2q}{m}}\,\frac{V^{3/2}}{s_c^2} \tag{5}$$

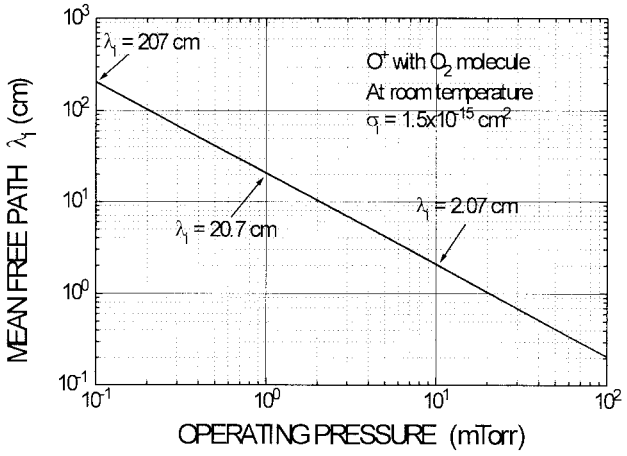

Fig. 5. Mean free path in an oxygen plasma versus the operating pressure.

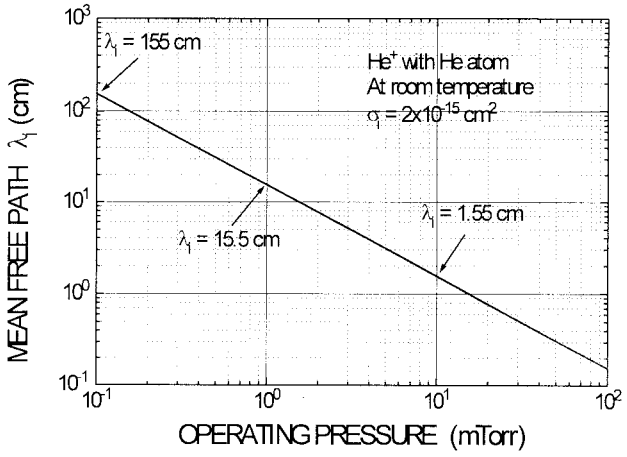

Fig. 6. Mean free path in a helium plasma versus the operating pressure.

and the implant dose-rate can be calculated by

$$\text{dose-rate} = j_c/q\ \left(/\text{cm}^2\ \text{s}\right). \tag{6}$$

Fig. 7 exhibits the steady-state sheath thickness versus the applied dc potentials for different ion densities. For a −50 kV dc potential, the sheath thicknesses are 52.4, 16.6, and 5.24 cm when the ion densities are 1×10^9, 1×10^{10}, $1\times10^{11}/\text{cm}^3$, respectively. When the ion density is $4\times10^9/\text{cm}^3$, as shown in Fig. 3, the sheath thickness is 26.2 cm. Fig. 8 shows the implant steady-state ion current versus dc biasing in an oxygen plasma for the different ion densities when the target is a 150-mm wafer. The ion current is independent of the applied potential. For a 150-mm wafer, the implant ion currents are 0.01, 0.101, and 1.01 A when the ion densities are 1×10^9, 1×10^{10}, $1\times10^{11}/\text{cm}^3$, respectively. The corresponding implant dose-rates are 3.46×10^{14}, 3.46×10^{15}, and $3.46\times10^{16}/\text{cm}^2\cdot\text{s}$ when the ion densities are 1×10^9, 1×10^{10}, $1\times10^{11}/\text{cm}^3$, respectively. When the ion density is $4\times10^9/\text{cm}^3$, as shown in Fig. 3, the implant ion current is 0.0404 A for a 150-mm wafer, and the corresponding implant dose-rate is $1.38\times10^{15}/\text{cm}^2\cdot\text{s}$. Fig. 9 shows the implant statistical ion current versus dc biasing in a helium plasma for the different ion densities when the target is a 150-mm wafer. Helium PIII yields a higher implant ion current because it has a lighter ion mass. Again, the implant ion current is independent of the applied potential. For a 150-mm wafer, the implant ion currents are

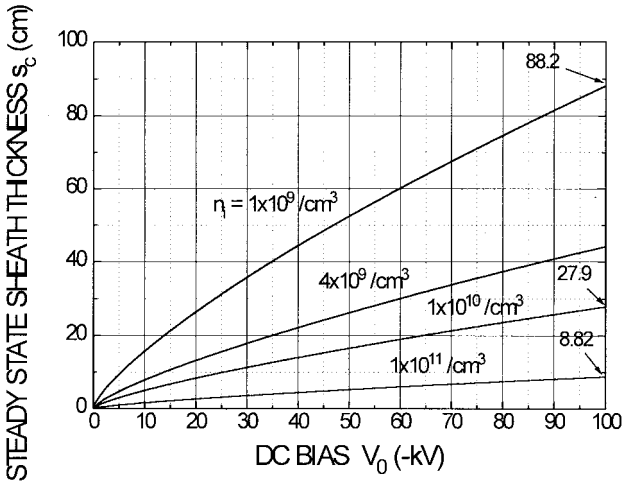

Fig. 7. Steady-state sheath thickness versus dc biasing for different ion densities.

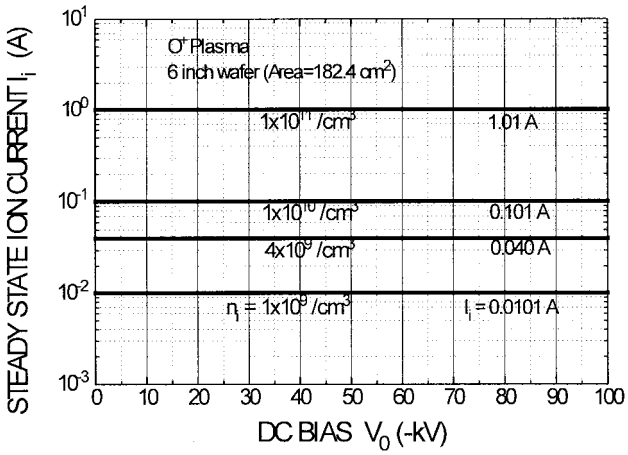

Fig. 8. Implant steady-state ion current versus dc biasing in an oxygen plasma for different ion densities when the target is a 150-mm (6-in) wafer.

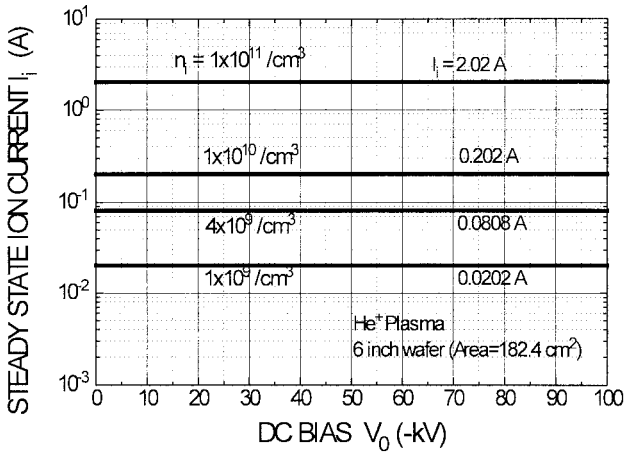

Fig. 9. Implant steady-state ion current versus dc biasing in a helium plasma for different ion densities when the target is a 150-mm (6-in) wafer.

0.02, 0.202, and 2.02 A when the ion densities are 1×10^9, 1×10^{10}, $1\times10^{11}/\text{cm}^3$, respectively. The corresponding implant dose-rates are 6.92×10^{14}, 6.92×10^{15}, and $6.92\times10^{16}/\text{cm}^2\cdot\text{s}$ when the ion densities are 1×10^9, 1×10^{10}, $1\times10^{11}/\text{cm}^3$, respectively. When the ion density is $4\times10^9/\text{cm}^3$, as shown in Fig. 3, the implant ion current is 0.081 A for a 150-mm wafer, and the corresponding dose-rate is $2.77\times10^{15}/\text{cm}^2\cdot\text{s}$. Table I summarizes the sheath thickness, ion currents, and dose rates of oxygen PIII (SPIMOX) and helium PIII (ion-cut) for different ion densities.

In order to optimize the SOI PIII process, several factors have to be seriously considered including working pressure, plasma density, plasma density uniformity, and system cost (chamber and power supply). All of them are relevant and may conflict with each other. For an optimal PIII system design (more compact and lower cost), a higher ion density is desired because a thinner sheath and higher implantation dose will result. However, there may be process limitations for high ion density PIII such as the collisionless requirement, overheating of the sample, maximum power output of the pulse generator, and degraded ion density uniformity. For example, a higher ion density equal to $\sim6\times10^9/\text{cm}^3$ can be obtained when the pressure is 2 mTorr (Fig. 4) and yields a better ion density uniformity (1.2%) for a 150-mm wafer. However, a worse ion density uniformity ($>20\%$) for a wafer size larger than 200 mm will result when using a pressure of 1 mTorr. We can assume that $s/\lambda_i<1$ is a criterion for the collisionless condition. From Fig. 7, the sheath thickness is $\sim$30 cm when the potential is -50 kV and ion density is $5\times10^9/\text{cm}^3$. However, the real sheath thickness is thinner if the two- or three-dimensional effects [17] are taken into account and is dependent on the process conditions as well as the ratio of sheath thickness scale and the target size. Under current conditions and a 150-mm wafer, the real sheath thickness is roughly half of the one-dimensional results, that is, $\sim$15 cm. The mean free paths at 2-mTorr pressure, shown in Figs. 5 and 6, are 10 and 8 cm for oxygen and helium plasmas, respectively. It does not satisfy the collisionless condition. When the pressure is 1-mTorr (Fig. 3), the ion density is $\sim4\times10^9/\text{cm}^3$ with a good density uniformity ($<4\%$) across a 400-mm wafer. As depicted in Figs. 5 and 6, the mean free paths at 1 mTorr pressure are 20 and 15.5 cm for oxygen and helium plasmas, respectively. They are larger than the sheath thickness (15 cm) so that the collisionless condition is satisfied.

A higher ion density and consequently a higher implant current density may cause two problems. They are overheating of the sample and the maximum output current of the power supply. Overheating of the sample during PIII must be avoided. The cost of the high-voltage dc power supply is significantly increased with the output power, which is determined by the product of the output voltage and current. The implant ion current is only a small fraction of the total implant current due to the secondary electron emission during PIII. The total implant current is $I_{\text{total}}=I_{io}\,(1+\gamma_i)$, where γ_i is the ion-impact secondary electron emission coefficient, which depends on the ion species, ion energy, target material, and target surface conditions. For instance, when the ion energy is 50 keV, γ_i are 2.4 and 3 for He^+ and O^+, respectively [18]. The total implant currents of 50-keV He^+ PIII will be 7, 0.7, and 0.07 A for a 150-mm wafer when the ion densities are 10^{11}, 10^{10}, and $10^9/\text{cm}^3$, respectively. When the ion density is $4\times10^9/\text{cm}^3$, the total implant currents of 0.164 and 0.280 A are required for SPIMOX (oxygen implant) and ion-cut (helium implant) processes. They are indeed big burdens for the high-voltage dc power supply.

ACKNOWLEDGMENT

Some of the SOI processes mentioned in this paper are based on pending patents of the University of California at Berkeley.

REFERENCES

[1] H. Vogt, G. Burbach, J. Belz, and G. Zimmer, "Silicon-on-insulator development in Europe," *Solid State Technol.*, vol. 34, no. 2, pp. 79–83, 1991.
[2] P. N. Dunn, "SOI: Ready to meet CMOS challenge," *Solid State Technol.*, vol. 36, no. 10, pp. 32–35, 1993.
[3] J.-P. Colinge, *Silicon-on-Insulator Technology: Materials to VLSI*. Boston, MA: Kluwer Academic, 1991.
[4] M. Bruel, "Application of hydrogen ion beams to silicon on insulator material technology," *Nucl. Instrum. Methods Phys. Res. B.*, vol. 108, pp. 313–319, 1996.
[5] J. V. Mantese, I. G. Brown, N. W. Cheung, and G. A. Collins, "Plasma immersion ion implantation," *MRS Bull.*, vol. 21, no. 8, pp. 52–56, 1996.
[6] P. K. Chu, N. W. Cheung, and C. Chan, "Recent applications of plasma immersion ion implantation," *Semiconductor Int.*, vol. 6, pp. 165–172, 1996.
[7] P. K. Chu, S. Qin, C. Chung, N. W. Cheung, and L. A. Larson, "Plasma immersion ion implantation—A fledgling technique for semiconductor processing," *Mat. Sci. Eng.: Reports*, vol. R17, nos. 6–7, pp. 207–280, 1996.
[8] J. Min, P. K. Chu, Y. C. Cheng, J. B. Liu, S. Im, S. Iyer, and N. W. Cheung, "Buried oxide formation by plasma immersion ion implantation," *Mat. Chem. Phys.*, vol. 40, no. 3, pp. 219–222, 1995.
[9] J. B. Liu, S. S. K. Iyer, C. M. Hu, N. W. Cheung, R. Gronsky, J. Min, and P. Chu, "Formation of buried oxide in silicon using separation by plasma implantation of oxygen (SPIMOX)," *Appl. Phys. Lett.*, vol. 67, no. 16, pp. 2361–2363, 1995.
[10] J. Min, P. K. Chu, Y. C. Cheng, J. Liu, S. S. Iyer, and N. W. Cheung, "Nucleation mechanism of SPIMOX (separation by plasma implantation of oxygen)," *Surf. Coat. Technol.*, vol. 85, pp. 60–63, 1996.
[11] X. Lu, S. S. K. Iyer, J. B. Liu, C. M. Hu, N. W. Cheung, J. Min, and P. K. Chu, "Separation by plasma implantation of oxygen to form silicon on insulator," *Appl. Phys. Lett.*, vol. 70, no. 13, pp. 1748–1750, 1997.
[12] P. K. Chu, X. Lu, S. S. K. Iyer, and N. W. Cheung, "A new way to make SOI wafers," *Solid State Technol.*, vol. 49, no. 5, pp. S9–S12, 1997.
[13] P. K. Chu, B. Y. Tang, Y. C. Cheng, and P. K. Ko, "Principles and characteristics of a new generation plasma immersion ion implanter," *Rev. Sci. Instrum.*, vol. 68, no. 4, pp. 1866–1874, 1997.
[14] S. S. K. Iyer, X. Lu, J. B. Liu, J. Min, Z. N. Fan, P. Chu, C. M. Hu, and N. W. Cheung, "Separation by plasma immersion of oxygen (SPIMOX) operational phase-space," *IEEE Trans. Plasma Sci.*, vol. 25, pp. 1128–1135, Oct. 1997.
[15] SOI Processing using PIII has patents pending, Univ. Calif. Berkeley.
[16] C. Chan, U.S. Patent 5 653 811.
[17] S. Qin, Y. Z. Zhou, and C. Chan, "Two-dimensional modeling and simulation for dynamic sheath expansion of plasma immersion ion implantation," *J. Appl. Phys.*, submitted 1997.
[18] S. C. Brown, *Basic Data of Plasma Physics*. Cambridge, MA: MIT Press, 1966, p. 233.

Paul K. Chu (M'97) received the B.S. degree in mathematics from the Ohio State University, Columbus, in 1977 and the M.S. and Ph.D. degrees in chemistry from Cornell University, Ithaca, NY, in 1979 and 1982, respectively.

He joined Charles Evans & Associates in California in 1982 and assumed various technical and managerial positions. He founded Evans Asia and became a Visiting Faculty Member of the City University of Hong Kong in 1990. He is currently Professor in the Department of Physics and Materials Science at the City University of Hong Kong, Professor in the Department of Computer Science at Peking University, China, and Advisory Professor in the Department of Materials Science at Fudan University, China. He is on the advisory board of a number of international scientific committees and organizations, and his current research interests are in plasma processing, electronic materials, and materials characterization.

Dr. Chu is a member of the American Chemical Society, Materials Research Society, and Böhmische Physical Society.

Shu Qin (M'95–SM'97) received the M.S. degree in electrical engineering from Qinghua (Tsinghua) University, Beijing, China, in 1982 and the Ph.D. degree in electrical engineering from Northeastern University, Boston, MA, in 1991.

From 1976 to 1979, he worked as a Research Engineer in the CAD Center of Qinghua University on VLSI design and processing. From 1982 to 1986, he worked as a Lecturer in the Beijing Institute of Posts and Telecommunications. From 1986 to 1987, he worked as a Research Scientist in the ECE Department, Lehigh University, Bethlehem, PA, on VLSI CAD. Since 1991, he has been with the Plasma Science and Microelectronics Lab, Northeastern University, Boston, MA, as a Research Scientist. His current research interests are advanced semiconductor processing, novel plasma sources, and device and process simulations. He holds two patents and has authored 80 technical papers in the areas of plasma processing, semiconductor fabrication, and microelectronics.

Chung Chan (S'78–M'81–SM'88–F'97) was born in Canton, China, on October 23, 1956. He received the B.S. degree in electrical engineering from North Dakota State University, Fargo, in 1978 and the M.S. and Ph.D. degrees in electrical and computer engineering from the University of Iowa, Iowa City, in 1980 and 1981, respectively.

From 1981 to 1984, he served as a Research Scientist at the Phaedrus Tandem Mirror, University of Wisconsin, Madison. In September 1984, he joined the Faculty of Northeastern University, Boston, MA, where he currently holds the title of Robert D. Black Professor of Electrical and Computer Engineering. He has published papers on topics related to novel plasma device, space plasma simulations, nonlinear plasma phenomena, plasma processing, microstructure fabrication, and novel plasma diagnostic techniques.

Nathan W. Cheung received the B.S. degree from the Massachusetts Institute of Technology, Cambridge, and the Ph.D. degree from the California Institute of Technology, Pasadena.

He is currently a Professor in the Department of Electrical Engineering and Computer Sciences at the University of California at Berkeley. His research activities include ion beam and plasma processing technologies, VLSI metallization, integrated circuit processing, integrated circuit reliability, and high bandgap semiconductors.

Dr. Cheung is a member of the American Electrochemical Society, American Vacuum Society, Materials Research Society, and Böhmische Physical Society.

Ping K. Ko (S'78–M'81–SM'93–F'96) was born in Hong Kong. He received the B.S. degree from Hong Kong University in 1974 and the Ph.D. degree from the University of California at Berkeley in 1982.

He was a Member of Technical Staff at Bell Labs from 1982 to 1983. He joined the UC Berkeley Faculty in 1984 and was Vice Chairman of the EECS Department before returning to Hong Kong in 1993. He is currently Dean of Engineering of the Hong Kong University of Science and Technology. His research interests include microelectronics technologies and devices and CAD tools for integrated circuits. He holds three patents and has authored or coauthored one book and more than 200 research papers.